

## CHAPTER-4

### A GENERALIZED MAGNETOHYDRODYNAMIC MODEL FORMALISM OF GRAVITATIONAL INSTABILITY IN SPHERICAL ASTROCLOUDS

***Abstract:** This Chapter offers a generalized magnetohydrodynamic (g-MHD) meanfluidic model theoretically constructed to analyze the gravitational instability dynamics excitable in a spherical complex astrocloud on the non-relativistic classical astroscales of space and time.<sup>†</sup> It concurrently includes the effects of viscoelasticity, buoyancy, polytropicity, volumetric thermal expansion, and so forth. A spherical normal mode analysis yields a unique form of a generalized linear cubic dispersion relation. It is interestingly found that the magnetic field in the presence of adopted non-ideality effects in the spherical astrocloud acts as a destabilizing agent. It sets out a new theoretic support to the existent various astronomic observations on the magnetic field acting as a cloud destabilizing agency in the presence of geometrical curvature (spherical) effects extensively reported in the literature.*

#### 4.1 INTRODUCTION

The dust molecular clouds (DMCs), well-known as the stellar nurseries, are featured with the physical properties of high density and low temperature relative to the background interstellar medium (ISM). The major constituents of such DMCs are heavy heterogeneous dust grains in the solid phase mixed-up with the gaseous phase of the interstellar hydrogen [1]. The dust is composed of graphite, silicate, and complex derivatives [2, 3]. The mean dust-to-gas ratio varies locally in the dense DMCs from the canonical ISM value of about 1% to the cloud value of 20-30% [4]. The variation of such dust abundance is amid various naturalistic dust accumulative processes, such as the Bondi accretion, Jeans accretion, and so on [2]. Besides, this dust enrichment is mainly due to the presence of larger grains (0.1  $\mu\text{m}$  grains by 10%, 10  $\mu\text{m}$  by 40%); and so forth [5]. Such DMCs undergo the self-gravitational collapse subjected to the threshold condition that the inward gravitational force beats the outward thermal force [1, 6]. This leads to the formation of diversified bounded structures such as, star, planets, dwarf stars and various compact astroobjects [1].

This instability has been extensively studied in the  $\text{H}_{\text{II}}$  region of DMCs [2, 3, 7-11]. The radiations from newly born stars or associated emission nebulae ionize the background

---

<sup>†</sup>Kalita, D. and Karmakar, P. K., Analyzing the instability dynamics of spherical complex astroclouds in a magnetized meanfluidic fabric. *Physics of Plasmas*, 27:022902. 1-9, 2020.

gas into plasmas ( $T \sim 10^4 \text{K}$ ). The contact electrification with the electron-ion thermal currents renders the grains electrically charged ( $Z_d \sim 10 - 10^4$ ) [2, 3, 7, 8]. The resulting long-range electric force modifies the Jeans instability into a new hybrid pulsational mode amid gravito-electrostatic coupling [9-11]. The Jeans threshold criterion and propagation dynamics is hugely affected due to the charged dust [9-11]. Such environs are confirmed to exist in the HII regions in the DMCs by the Hubble space telescope [2, 3, 7, 8].

The charged dust in the DMCs is a strongly coupled state with a higher Coulomb coupling parameter [ $\Gamma_{Cou} = (1/4\pi\epsilon_0)\{(Z_d e)^2 / (ak_B T_d)\} \gg 1$ ] [12, 13]. Here,  $a = (3/4\pi n_d)^{1/3}$  is the Wigner-Seitz radius of the constitutive identical solid dust grains.  $n_d$  is the non-equilibrium dust number density. In the regime,  $1 \leq \Gamma_{Cou} \leq 160$ , the dust fluid shows “viscoelasticity” [12]. It hereby exhibits simultaneously the properties of both liquid and solid in a generalized hydrodynamic (GH) landscape. Their conjoint conjugate action results in the excitation of a rich spectrum of collective oscillations, waves and instabilities [14-17]. To name a few, such instability classes include the viscoelastic relaxation instability [15], viscoelastic pulsational instability mode [17], gravito-acoustic instability [18], Buneman instability [19], Kelvin-Helmholtz (shear) instability [20], and so forth.

The Jeans instability problem has been widely addressed in different astronomical viscoelastic fluid media in plane parallel geometry in the past, both in the linear [14, 16, 17] and nonlinear [18] regimes. It has been found that the viscoelastic relaxation time stabilizes the instability in the linear regime (Chapter-2). But, it goes opposite in the non-linear regime (Chapter-3). The fluid viscosity has been found to stabilize the astrofluid system in both the cases. It is realistically relevant to various astrostructures and environs, such as the neutron stars, dwarf stars, planetary disks, planetary interiors, and so forth [21, 22]. Clearly, there has been a great long-sought model necessity for the inclusion of fluid viscoelastic properties in non-planar geometry as per the realistic spherical magnetized DMCs amid all the possible key electromagnetic fluid dynamical effects [1, 23].

In this Chapter, we consider an astronomical situation comprising of a spherically symmetric magnetized viscoelastic polytropic DMC treated in the framework of a generalized magnetohydrodynamic ( $g$ -MHD [24]) model. The goal is to see the excitation dynamics of gravitational instability on the non-relativistic classical astrofluidic scales of space and time. The spherical geometry consideration is due to the fact that the astrofluidic clouds (DMCs) are usually spherical in geometric shape against the traditionally treated

simplified planar ones [25, 26]. Examples are the Lagoon Nebula (M8) and Trifid Nebula (M20) in Sagittarius, Rosette Nebula (NGC 244) in Monoceros, and, so forth [1]. A standard technique of spherical wave analysis [27, 28] over the cloud results in a unique form of a generalized cubic linear dispersion relation. A numerical illustrative scheme, after the Cardan cubic decomposition method [29], reveals the key stabilizing and destabilizing factors for the first time. The temperature, polytropicity, viscoelastic relaxation time, effective viscosity and cloud size act as stabilizing factors. The mean constitutive mass and magnetic field act as destabilizing influential sources against the gravity. It is herewith interestingly conjectured that the field moderated with the diversified non-ideality effects destabilizes the spherical (non-planar) DMC. It is against the typical stability picture in the magnetized ideal case [30-33]. It is in fair agreement with the past astronomic observations that the measured magnetic pressure field is weaker than the cloud self-gravitational pressure field in a spherical geometry against the traditional field-stabilizing picture of planar (flat sheet-like) DMCs [30, 31]. The relevancy of our investigated non-trivial results in the inhomogeneous global cloud fragmentation instability triggering local bounded astrostructure formation is finally outlined.

## 4.2 PHYSICAL MODEL AND FORMALISM

We consider an astronomical star-forming situation constituted of magnetized spherical polytropic viscoelastic DMC in the  $g$ -MHD framework. It is microscopically composed of tiny electrons and ions (both weakly coupled species) and negatively charged heavier dust particulates (strongly coupled). Thus, it is only the dust fluid that has high collective correlation (Coulombic) against the mutualistic thermal interplay (randomizing). When the dimension of the DMC ( $L$ ) in the ISM is much larger than its plasma Debye length ( $\lambda_D$ ), the dust-plasma system is treated as a globally quasi-neutral fluid. In our considered model, we estimate  $L \geq 1.3 \times 10^6$  m and  $\lambda_D = 6.9 \times 10^{-3}$  m, thereby implying a quasi-neutral DMC approximation as a well validated one. All the judicious inputs used in the estimation are discussed later in the numerical analysis. The quasi-neutrality condition allows the constitutive multicomponent fluids to evolve collectively as a single meanfluid landscape based on the small mean-free path approximation [34]. A non-relativistic approach is sought herein because of the relatively small magnitude of the meanfluidic flow velocity on the non-relativistic classical astrofluidic scales of space and time. The plasma flow speed

( $c_s \approx 0.12 \text{ m s}^{-1}$ ) is indeed too small for the relativistic effects [33]. Such astrofluids get unstable against the perturbations of all wavelengths due to the inward self-gravity [25, 28].

It is pertinent to add that the physical processes responsible behind the various dust-dust interactions (e.g., direct bombardment, Coulomb scattering and Coulomb attraction-repulsion forces) in various dusty plasma configurations are highly scale-dependent in nature [35-37]. The Coulomb interactions among the dust grains in a vast partially ionized dusty plasma is well known to affect the pure Jeans instability mode significantly by introducing an impure hybrid gravito-electrostatic pulsating mode [9, 10]. In the present case dealing with the fully ionized dusty plasma configurations in the meanfluidic approximation on the astrophysical spatiotemporal scales however, the collective dust-dust interaction mechanisms are fully averaged out. As a consequence, the consideration of the Coulombic interactions among the constitutive massive dust grains on the astrophysical spatiotemporal scales is physically irrelevant in the present astronomic backdrop.

In our model, the Coulomb coupling parameter for the dust-dust interaction is  $\Gamma_{Cou} = 1.25 \times 10^{-6} \times Z_d^2 = 1.25 \times 10^2$  [12, 13]. It is well in the critical domain [12, 13], which is needed for the fluid viscoelasticity as,  $1 \leq \Gamma_{Cou} \leq 160$ . When  $\Gamma_{Cou} > 1$ , the relaxation time is as,  $\tau_m < \omega_p^{-1}$ ; where,  $\omega_p \tau_m \approx \Gamma_{Cou}^{-3/2} \ll 1$  [38]. This collision-dominated situation links to the "hydrodynamic continuum regime", thereby validating the present  $g$ -MHD to use.

We apply the non-Newtonian (Maxwellian) fluidic formalism to monitor the DMC-dynamics on the relevant spatiotemporal scales. It is accordingly portrayed in a spherically symmetric coordinate system ( $r, t$ ) in a usual meanfluidic  $g$ -MHD shape as

$$\frac{\partial \rho}{\partial t} + \frac{1}{r^2} \frac{\partial}{\partial r} (r^2 \rho v_r) = 0, \quad (4.1)$$

which is the continuity equation stating the fluid constitutive particle flux-density conservation law [38-41]. The meanfluid velocity is  $v_r$  and mean density is  $\rho$ .

The momentum equation for the force-density conservation includes concurrently the gravity, buoyancy, and azimuthal magnetic field  $\vec{B} = (0\hat{r} + 0\hat{\theta} + B_\phi \hat{\phi}) \equiv (0, 0, B_\phi)$  as

$$\begin{aligned} & \left\{ 1 + \tau_m \left( \frac{\partial}{\partial t} + v_r \frac{\partial}{\partial r} \right) \right\} \left\{ \rho \left( \frac{\partial}{\partial t} + v_r \frac{\partial}{\partial r} \right) v_r + \frac{c_s^2}{\Gamma} \frac{\partial \rho}{\partial r} + \rho (1 + \gamma T) \frac{\partial \psi}{\partial r} + \frac{B_\phi}{\mu_0 r} \frac{\partial}{\partial r} (r B_\phi) \right\} \\ & = \left( \varsigma + \frac{4}{3} \eta \right) \left\{ \frac{\partial^2 v_r}{\partial r^2} + \left( \frac{2}{r} \right) \frac{\partial v_r}{\partial r} \right\} - 2 \left( \varsigma + \frac{1}{3} \eta \right) \frac{v_r}{r^2}, \end{aligned} \quad (4.2)$$

where,  $\tau_m$  is the viscoelastic relaxation time (causing memory effects),  $\Gamma = 1 + n_p^{-1}$  is the polytropic exponent (typifying cloud-centric mass condensation) with  $n_p$  is the polytropic index,  $\gamma$  is the coefficient of volumetric expansion (thermal expansion).  $\eta$  and  $\zeta$  are the shear viscosity (first viscosity, resistance to flow) and bulk viscosity (second viscosity, resistance to volumetric expansion) in the unnormalized (dimensional) form, respectively.  $\psi$  is the self-gravitational potential developed due to the fluid material density field.  $T$  is the meanfluidic temperature (in Kelvin, K).  $c_s = (\Gamma Z_d k_B T / m)^{1/2}$  is the normal sound phase speed. The mean mass of the constitutive particles is  $m$ . The meanfluidic approach to derive the momentum equation is described in the Appendix-4.A.

It is noteworthy that, in the meanfluidic approach of the current interest, the various heterogeneous collisional processes between the constitutive massive dust grains and other lighter constitutive species are averaged out to a net-zero momentum exchange in the dust meanfluidic frame of reference [42]. As a consequence, no conventional collisional momentum exchange terms are retained in the momentum equation (equation (4.2)) in the current  $g$ -MHD framework. In contrast, the different collisional exchange terms could be present in the various constitutive momentum equations describable in the fabric of a multifluidic formalism instead of the presented  $g$ -MHD framework. Such approaches have widely been reliably applied in various astrophysical and space environments with no violation of any generality in the past [42].

In this adopted meanfluidic formalism, the basic postulate inherent in equation (4.2) is that  $\eta$  and  $\zeta$  do not spatiotemporally change on the scales of our observation. Now,  $\eta$  and  $\zeta$  in terms of the known plasma parameters are respectively given [13, 38] as

$$\eta = \eta^* (nm\omega_p a^2), \quad (4.3)$$

$$\zeta = -\frac{4}{3}\eta + \zeta^* (nm\omega_p a^2), \quad (4.4)$$

where,  $\eta^*$  and  $\zeta^*$  are the reduced kinematic shear viscosity and reduced kinematic bulk viscosity in the normalized (non-dimensional) form [38] given, respectively, as

$$\eta^* = \frac{1}{15} \left( \frac{3\pi}{2} \right)^{\frac{1}{2}} \left( \frac{5}{\Gamma_{Cou}} - I_1 \right)^{\frac{3}{2}} \left( \frac{17}{\Gamma_{Cou}} + 8I_{-2} + \frac{81}{10}H_3 + \frac{39}{10}H_1 \right)^{\frac{1}{2}}, \quad (4.5)$$

$$\zeta^* = \frac{1}{15} \left( \frac{\pi}{2} \right)^{\frac{1}{2}} \left( \frac{15}{\Gamma_{Cou}} + 2I_1 - 15\gamma_{sp} d \right)^{\frac{3}{2}} \left( \frac{7}{\Gamma_{Cou}} + \frac{14}{3}I_{-2} + \frac{18}{5}H_3 + \frac{17}{5}H_1 \right)^{\frac{1}{2}}. \quad (4.6)$$

Here,  $\gamma_{sp} = c_p / c_v$  is the ratio of the specific heat at constant pressure ( $c_p$ ) to that at constant volume ( $c_v$ ) [13, 38].  $k_T^0 = (nk_B T)^{-1}$  denotes the isothermal ideal gas compressibility.  $K_T = (1/\rho)(\partial\rho/\partial P)_T = (nk_B T)^{-1}\{-(1/9)(c_v/Nk_B) + (4/3)(U/Nk_B T)\}^{-1}$  is the isothermal generalized meanfluidic compressibility.  $U$  is the excess internal energy of the fluid system [39].  $d = \{1/(3\Gamma_{Cou})\}(K_T^0/K_T)$  is a dimensionless quantity which interrelates the Coulomb coupling parameter and these compressibilities. The different numerical values of the above standard integrals  $I_1, I_{-2}, H_1, H_3$  are tabulated for the varied  $\Gamma_{Cou}$ -values, derived from extensive molecular dynamics simulations, but founded on statistical approach [38].

The electromagnetic induction equation governs the magnetic field-line evolution with the  $g$ -MHD wave propagation dynamics in the usual notations [40] as

$$\frac{\partial B_\phi}{\partial t} + \frac{1}{r} \frac{\partial}{\partial r} (r v_r B_\phi) = 0. \quad (4.7)$$

The polytropic equation of state relates the pressure ( $P$ ) with density ( $\rho$ ) expressing a perfect balance between the DMC heating-cooling processes [41], given as

$$P = K_p \rho^\Gamma, \quad (4.8)$$

where,  $K_p$  denotes the polytropic constant of the astrofluid as a polytrope.

The self-gravitational Poisson equation relates the gravitational potential evolution with the material density distribution in space locally given as

$$\frac{1}{r^2} \frac{\partial}{\partial r} \left( r^2 \frac{\partial \psi}{\partial r} \right) = 4\pi G \rho. \quad (4.9)$$

Thus, the complex meanfluidic dynamics of the spherical DMC in the  $g$ -MHD framework of our interest is concurrently governed by equations (4.1)-(4.2), (4.7)-(4.9) as a closed dynamical system.

The main goal of this Chapter is to see the stability of the considered spherical DMC in non-relativistic domain. So, we allow the relevant parameters ( $F$ ) depicting the spherical DMC undergo small-scale (linear) perturbation [43, 44] ( $F_1$ ) relative to their homogeneous equilibrium values ( $F_0, F \gg F_1$ ) as

$$F(r, t) = F_0 + F_1 \left( \frac{1}{r} \right) \exp[-i(\omega t - kr)], \quad (4.10)$$

$$F = [\rho \quad v_r \quad P \quad T \quad \psi \quad B_\phi]^T, \quad (4.11)$$

$$F_0 = [\rho_0 \ 0 \ P_0 \ T_0 \ 0 \ B_{\phi 0}]^T, \quad (4.12)$$

$$F_1 = [\rho_1 \ v_{r1} \ P_1 \ T_1 \ \psi_1 \ B_{\phi 1}]^T, \quad (4.13)$$

where,  $\omega$  is the angular frequency and  $k$  is the angular wavenumber of the fluctuations in the unnormalized form. The symbol “[ $\ ]^T$ ” here represents the “transpose” of the matrix “[ $\ ]$ ”.

Use of equations (4.10)-(4.13) yields  $\partial/\partial r \rightarrow (ik - r^{-1})$ ,  $\partial/\partial t \rightarrow (-i\omega)$  and  $\partial^2/\partial r^2 \rightarrow [(-k^2 + 2r^{-2}) - i(2kr^{-1})]$ . In the new  $(k, \omega)$ -space, equations (4.1)-(4.2), (4.7)-(4.9) respectively read as

$$\left( ik + \frac{1}{r} \right) \rho_0 v_{r1} = i\omega \rho_1, \quad (4.14)$$

$$\begin{aligned} (1 - i\omega\tau_m) & \left[ -i\omega \rho_0 v_{r1} + \left( ik - \frac{1}{r} \right) \left\{ \frac{c_s^2}{\Gamma} \rho_1 + \rho_0 (1 + \gamma T_0) \psi_1 + \frac{B_{\phi 0} B_{\phi 1}}{\mu_0} \right\} + \frac{2B_{\phi 0} B_{\phi 1}}{\mu_0 r} \right] \\ & = -k^2 \left( \varsigma + \frac{4}{3} \eta \right) v_{r1} - 2 \left( \varsigma + \frac{1}{3} \eta \right) \frac{v_{r1}}{r^2}, \end{aligned} \quad (4.15)$$

$$B_{\phi 1} = \frac{k}{\omega} B_{\phi 0} v_{r1}, \quad (4.16)$$

$$P_1 = K_p \Gamma \rho_0^{\Gamma-1} \rho_1, \quad (4.17)$$

$$\psi_1 = -\frac{4\pi G}{k^2} \rho_{d1}. \quad (4.18)$$

A standard procedure of decomposition and elimination in equations (4.14)-(4.18) results in a generalized cubic dispersion relation amid geometric curvature effects as

$$\begin{aligned} \omega^3 + \left[ \left\{ -\frac{c_s^2}{\Gamma} + (1 + \gamma T_0) \frac{\omega_J^2}{k^2} \right\} \left( k^2 + \frac{1}{r^2} \right) - v_A^2 k^2 - \frac{k^2}{\tau_m \rho_0} \left\{ \chi + (\chi - \eta) \frac{2}{k^2 r^2} \right\} \right] \omega \\ - \left( \frac{v_A^2 k}{\tau_m} \right) \frac{1}{r} = 0, \end{aligned} \quad (4.19)$$

where,  $\chi = \varsigma + (4/3)\eta$  is the effective generalized (composite) meanfluidic viscosity and  $v_A = B_{\phi 0} (\mu_0 \rho_0)^{-1/2}$  is the Alfvén wave phase velocity in the  $g$ -MHD approach.

After a standard astronomical normalization scheme [14, 16], equation (4.19) is standardized from the old Fourier space  $(k, \omega)$  into the new one  $(K, \Omega)$ , cast as

$$\Omega^3 + \left[ \left\{ -\frac{1}{\Gamma} + \frac{(1 + \gamma T_0)}{K^2} \right\} \left( K^2 + \frac{1}{\xi^2} \right) - \left( \frac{v_A^2}{c_s^2} \right) K^2 - \frac{K^2}{c_s^2 \rho_0 \tau_m} \left\{ \chi + \frac{2}{K^2 \xi^2} (\chi - \eta) \right\} \right] \Omega$$

$$-\left(\frac{v_A^2 K}{c_s^2 \omega_j \tau_m}\right) \frac{1}{\xi} = 0. \quad (4.20)$$

Here,  $\xi = r/\lambda_j$  is the Jeans-normalized radial distance relative to the cloud centre.  $\Omega = \omega/\omega_j$  and  $K = k/k_j$  are the Jeans-normalized angular frequency and wavenumber, respectively.

The mathematical construct of equation (4.20) reveals an interesting fact that the oversimplified cloud fluctuations in a field-free planar geometry ( $\xi \rightarrow \infty$ ,  $Z_d \rightarrow 1$ ,  $B_{\phi 0} \rightarrow 0$ ) would experience resonant growths if  $(1 + \gamma T_0) > [(K^2/\Gamma)[1 + \{\chi/(n_0 \tau_m k_B T_0)\}]]$ .  $n_0 = \rho_0/m$  is the equilibrium number density of the constitutive particles. So, equation (4.20) now reduces as

$$\Omega = \left\{ \frac{K^2}{\Gamma} \left( 1 + \frac{\chi}{n_0 \tau_m k_B T_0} \right) - (1 + \gamma T_0) \right\}^{\frac{1}{2}}, \quad (4.21)$$

which is in fair agreement with the previous dispersion results on the viscoelastic Jeans instability as in Chapter-2 of this thesis. Besides, equation (4.20) is similar to the reduced cubic form of the Cardan polynomial [29] given in a regular standard fashion as

$$\Omega^3 + 3\alpha\Omega + 2\beta = 0, \quad (4.22)$$

where, the various coefficients appearing in equation (4.22) are given respectively as

$$3\alpha = \left\{ -\frac{1}{\Gamma} + \frac{(1 + \gamma T_0)}{K^2} \right\} \left( K^2 + \frac{1}{\xi^2} \right) - \left( \frac{v_A^2}{c_s^2} \right) K^2 - \frac{K^2}{c_s^2 \rho_0 \tau_m} \left\{ \chi + \frac{2}{K^2 \xi^2} (\chi - \eta) \right\}, \quad (4.23)$$

$$2\beta = -\left( \frac{v_A^2 K}{\omega_j c_s^2 \tau_m} \right) \frac{1}{\xi}. \quad (4.24)$$

The macroscopic fluid dynamics, as obtained by the Cardan method [29], is governed only by the sensible dispersion root with positive imaginary part (any  $\Omega_r$ , but  $\Omega_i > 0$ ) given as

$$\Omega = (\Omega_r + i \Omega_i) = -\frac{1}{2}(u_1 + v_1) + i \frac{\sqrt{3}}{2}(u_1 - v_1), \quad (4.25)$$

where, the unknowns  $(u_1, v_1)$  in equation (4.25), with the corresponding predefined factors  $(\alpha, \beta)$  in equations (4.23)-(4.24), are respectively defined as

$$u_1 = \left\{ -\beta + (\beta^2 + \alpha^3)^{1/2} \right\}^{1/3}, \quad (4.26)$$

$$v_1 = \left\{ -\beta - (\beta^2 + \alpha^3)^{1/2} \right\}^{1/3}. \quad (4.27)$$



Clearly, equation (4.25) can be employed to see the dispersion features of the instability in the spherical DMC. The free energy source for exciting the instability onset obviously arises from the combined action of the buoyancy, gravitational energy, and plasma currents self-consistently driven via the inhomogeneous  $g$ -MHD convective flow dynamics.

### 4.3 RESULTS AND DISCUSSIONS

A theoretic model for the stability of a complex magnetized self-gravitating spherical DMC in the  $g$ -MHD framework is proposed. It considers the important fluid properties, such as the buoyancy, polytropicity and viscoelasticity in a spherically symmetric geometry. A Fourier-based spherical wave analysis over the DMC results in a cubic linear dispersion relation. It is analyzed numerically to see the instability features as in figures 4.1-4.8.

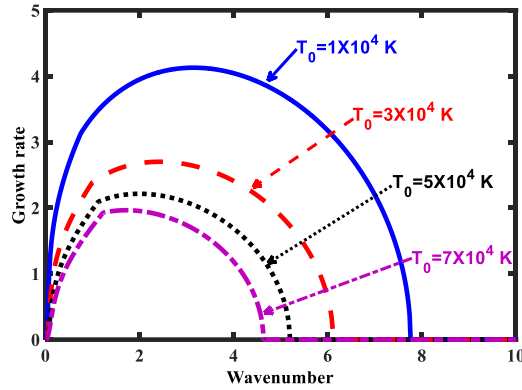


**Figure 4.1:** Profile of the Jeans-normalized growth rate ( $\Omega_i$ ) of the fluctuations with variation in the Jeans-normalized wavenumber ( $K$ ) for the different  $T_0$  – values.

In figure 4.1, the profiles of the Jeans-normalized instability growth rate ( $\Omega_i$ ) with variation in the Jeans-normalized wavenumber ( $K$ ) at different equilibrium temperatures ( $T_0$ ) are depicted. The different inputs used in the analysis are adopted from various reliable sources available in the literature [1, 3, 23, 25, 38, 45]. We now quantify the input properties of the constitutive (dust) particles [3, 25, 45] as  $m = 10^{-13}$  kg,  $n_0 = 10^8$  m<sup>-3</sup>,  $\rho_0 = 10^{-5}$  kg m<sup>-3</sup> and  $Z_d = 10^4$  at  $\xi = 10$ . The other inputs are  $\chi = 1.0 \times 10^{-10}$  kg m<sup>-1</sup> s<sup>-1</sup> [38];  $\tau_m = 10^{-3}$  s,  $\Gamma = 1$  [38];  $B_{\phi 0} = 10^{-10}$  T [1, 23]; and  $\gamma = 10^{-4}$  K<sup>-1</sup> [46]. It is seen that, as  $T_0$  increases,  $\Omega_i$  decreases, and vice-versa. It is attributable to the fact that, as  $T_0$  increases, the thermal outward pressure increases, and vice-versa. In other words, the fluid exerts the thermal

randomizing pressure (outward) in an anti-cloud-centric direction, thereby, preventing the spherical DMC to collapse against the organizing gravity (inward). Thus,  $T_0$  acts as a stabilizing agent against the DMC. So, the hotter the cloud, the more stable it is against the gravity, and vice-versa.

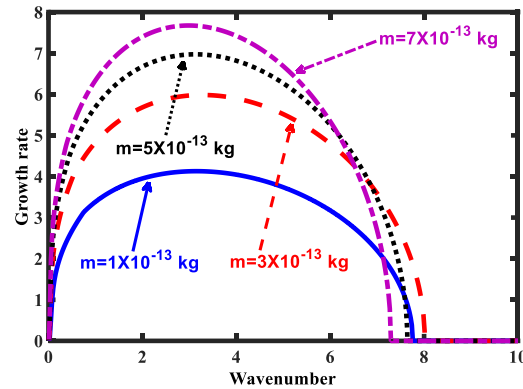


**Figure 4.2:** Same as figure 4.1, but with a fixed  $T_0 = 1 \times 10^4$  K for different  $m$  – values.

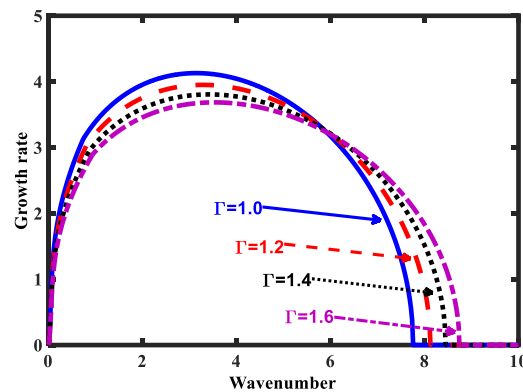


**Figure 4.3:** Same as figure 4.1, but with a fixed  $T_0 = 1 \times 10^4$  K for different  $\Gamma$  – values.

In figure 4.2, we show the same as figure 4.1, but with variation in the mean constitutive particle mass ( $m$ ) at fixed  $T_0 = 10^4$  K. It is seen that, as  $m$  increases,  $\Omega_i$  increases, and vice-versa. As  $m$  increases, the cloud becomes heavier, and vice-versa. A dynamical state is reached when the inward gravitational pull exceeds the resultant outward cloud pressure. So, an enhanced  $m$  results in a destabilizing influence, thereby paving the way for the cloud collapse to occur. So,  $m$  acts as a destabilizing agent to the magnetoactive collapse dynamics against gravity.

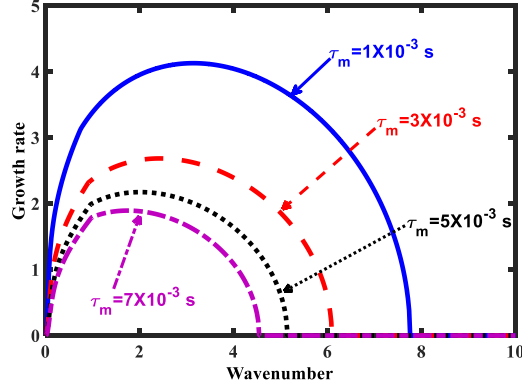


**Figure 4.4:** Same as figure 4.1, but with a fixed  $T_0 = 1 \times 10^4$  K for different  $\tau_m$  - values.

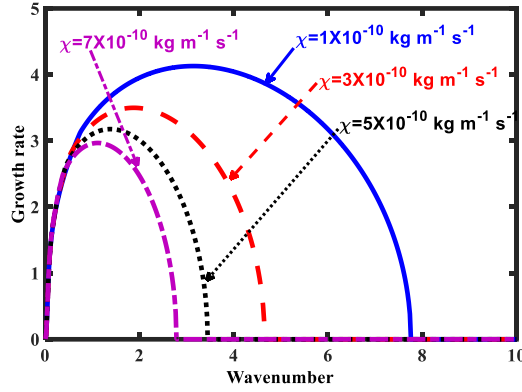


**Figure 4.5:** Same as figure 4.1, but with a fixed  $T_0 = 1 \times 10^4$  K for different  $\chi$  - values.

As in figure 4.3, we display the same as figure 4.1, but at fixed  $T_0 = 10^4$  K for the different  $\Gamma$ -values. It is seen here that, as  $\Gamma$  increases,  $\Omega_i$  decreases, and vice-versa. In other words, the polytropic exponent,  $\Gamma$ , acts as a stabilizing agent. It is attributable mainly to the fact that the deviation from the thermalized configuration ( $\Gamma \approx 1$ , isothermal, optically thin [47]) towards the non-thermal one ( $\Gamma > 1$ , non-isothermal, optically thick [47]) develops anti-cloud-centric randomizing forces, thereby preventing the cloud collapse. In other words, the cloud undergoes a dynamic transformation from an unstable (former) to a stable (latter) configuration.

In figure 4.4, we portray the same as figure 4.1, but at fixed  $T_0 = 10^4$  K for the different  $\tau_m$ -values. It is seen that, with increase in  $\tau_m$ ,  $\Omega_i$  decreases, and vice-versa. The long-range gravitational force (inward) fails to boost up the cloud collapse against the

strong restoring elastic force (outward). Thus,  $\tau_m$  acts as a stabilizing agent to the cloud dynamics against the mutualistic gravitoelastic interplay (counteracting).

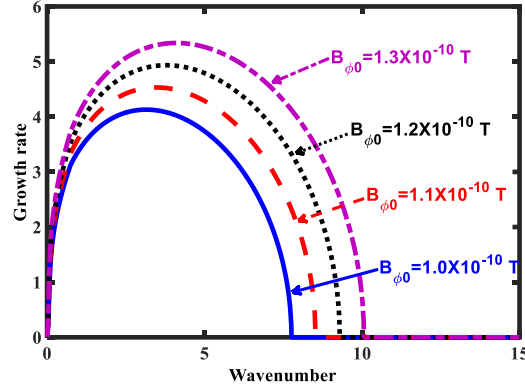


**Figure 4.6:** Same as figure 4.1, but with a fixed  $T_0 = 1 \times 10^4$  K for different  $B_{\phi_0}$  - values.

As in figure 4.5, we show the same as figure 4.1, but at  $T_0 = 10^4$  K (fixed) for the different  $\chi$  - values. As the  $\chi$  - value increases, the  $\Omega_i$  - value decreases, and vice-versa. With increase in  $\chi$ , the mean cohesive force among the major constituents increases, thereby restricting the fluid motion to a considerable extent. As a result, the meanfluidic system tends to a greater stability against the inward gravity and any other like possible operative forces. Thus,  $\chi$  acts as a stabilizing agent to the fluctuation dynamics against the self-gravitational cloud collapse.

As in figure 4.6, we depict the same as figure 4.1, but at  $T_0 = 10^4$  K (fixed) for the different  $B_{\phi_0}$  -values. As the  $B_{\phi_0}$  -value increases,  $\Omega_i$  increases; and vice-versa. If the  $B_{\phi_0}$  -strength increases in magnitude, the geometric curvature of the magnetic field lines increases, thereby contributing to the enhanced hoop stress, also termed as magnetic tension [42, 48]. As a result, it exerts more radially inward (cloud-centric) force. In the real interstellar circumstances,  $B_{\phi_0} \approx 10^{-10}$  T, which is a considerably weak field [1, 23]. So, the conservative non-local gravitational force (inward, destabilizing) due to the highly populated constituent particles [25, 45] ( $n_0 \approx 10^8$  m<sup>-3</sup>) in the spherical DMC beats over the non-conservative local magnetic tensile action (outward, stabilizing) in the presence of strong geometric curvature moderation. Due to the conjoint action of the complex gravito-magnetic interplay, the moderated magnetic field acts as a destabilizing agent to the spherical DMC fluctuations – an unusual behaviour of the magnetic field in the presence of

ambipolar diffusion – as previously reported elsewhere [4, 30, 31, 33, 49]. Interestingly, it is against the conventional picture of the DMC stabilization against the self-gravity action [30, 31]. The magnetic field-destabilizing the spherical DMC is in full agreement with the previous astronomic observations experimented with the Zeeman effects [30, 50, 51].

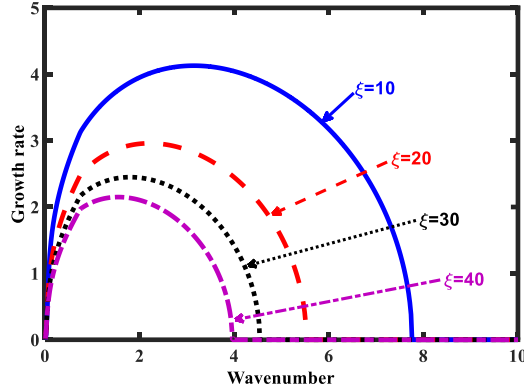


**Figure 4.7:** Same as figure 4.1, but with a fixed  $T_0 = 1 \times 10^4$  K for different  $\xi$  – values.

In figure 4.7, we display the same as figure 4.1, but at  $T_0 = 10^4$  K (fixed) for the different  $\xi$ -values. As the  $\xi$ -value increases for a given cloud (of fixed mass, population, temperature, etc.), the  $\Omega_i$ -value decreases, and vice-versa. Thus,  $\xi$  acts a stabilizing agent to the spherical DMC against the self-gravity. It is attributable to the universal Newtonian picture of the long-range (inverse square) self-gravity (cloud-centric), which decreases with the interparticle separation in the DMC in a given thermodynamic environ. In other words, it happens due to the well-known fact that the cloud self-gravitational pressure force decreases with increase in size, and vice-versa. Again, for bigger clouds, only the long (short)-wavelength perturbations undergo resonant-type of growths (decays), thereby rendering the cloud gravitationally unstable (stable). Such stabilizing effects caused by the geometric curvature radius (i.e., deviation from the plane-parallel geometry) are quite bolstered with the previous reports in similar astrophysical isothermal gaseous fluids enclosed in spherical shells [52].

Lastly, as in figure 4.8, we display the 3-D spatio-spectral pattern of figure 4.7, with  $\xi$  as a new variable with the inputs as before. As in figure 4.7,  $\Omega_i$ , here too, decreases with  $\xi$ , and vice-versa. Interestingly, for a given DMC, the  $\Omega_i$ -behaviour is prominent only in the gravitational regime (low- $K$ ); but, not so in the acoustic one (high- $K$ ). The remaining

features are the same as the previous case (figure 4.7). It may be inferred herein that the central part of the spherical DMC is the most unstable zone against the non-local self-gravity. As one moves radially outwards, the cloud acquires a unique propensity to become more and more stable against the self-gravity. It is seen further that, all the constitutive parts of the DMC are not regularly and uniformly sensitive to the applied local perturbations (figure 4.8), leading to the global DMC fragmentation.

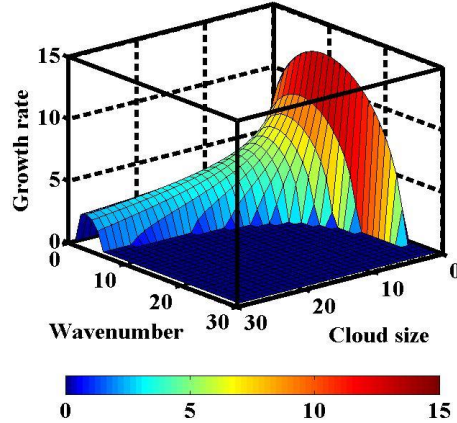


**Figure 4.8:** Profile of the Jeans-normalized growth rate ( $\Omega_i$ ) of the fluctuations with conjoint variation in the Jeans-normalized wavenumber ( $K$ ) and Jeans-normalized radial cloud size ( $\xi$ ).

#### 4.4 CONCLUSIONS

A semi-analytic investigation is systemically carried out to see the gravitational instability behaviour of a spherically symmetric astrocloud (DMC) in the presence of the combined action of possible realistic dynamical factors. It considers the fluid viscoelasticity, polytropicity, fluid buoyancy and azimuthal (toroidal) magnetic field simultaneously. It is in the framework of a standard  $g$ -MHD meanfluidic model dynamically evolving on the non-relativistic classical astrofluidic scales of space and time. The basic set of the governing equations describing the fluid dynamical evolution is developed as a coupled dynamical system. The fluid is initially assumed to be in a magnetohydrostatic homogeneous equilibrium. Around it, small-scale perturbations (linear) are applied. Application of spherical wave analysis reduces the perturbed DMC into a unique generalized cubic linear dispersion relation. It transforms the model system into a simple algebraic form of the standard Cardan polynomial for executing the stability solvability.

A constructive numerical analysis over the Cardan-decomposed polynomial roots is systemically carried out to explore the various instability stabilizing and destabilizing factors. It is found that the meanfluidic temperature, polytropicity, viscoelastic relaxation time, effective generalized viscosity and radial cloud size act as active stabilizing factors against the self-gravity action. In contrast, the constitutive mass and magnetic field act as destabilizing agents against the canonical Jeans collapse. Besides, an increment in the cloud constitutive mass, effective generalized viscosity and radial cloud size causes the long wavelength fluctuations to undergo active growth noticeably. In contrast, an increment in the meanfluidic temperature, polytropicity, viscoelastic relaxation time and magnetic field renders the gravito-magneto-acoustic instability to grow in the acoustic range alone. It is theoretically seen for the first time that the magnetic field acts as the cloud destabilizer, which is in accord with the previous astronomic observations, experimentally centred on the Zeeman effect [30, 50, 51]. Clearly, it is a novel result caused due to the concurrent action of the diversified non-ideal meanfluidic factors in the curved (spherical) geometry, causing the field lines to curve (as if, induced by ambipolar diffusion phenomena [30]).

In summary the key dynamical features of the collective correlative instability dynamics of the self-gravitating astrofluid are elaborately analyzed in a non-relativistic classical  $g$ -MHD formalism. The various stabilizing and destabilizing factors of the DMC against the self-gravity are identified and characterized. This analysis can enable us to see the collective wave-instability processes towards the compact structure formation and their correlated atmospheres, such as neutron stars, white dwarfs, planetary dense interiors, etc.

## REFERENCES

- [1] Kutner, M. L. *Astronomy: A Physical Perspective*. Cambridge University Press, Cambridge, 2003.
- [2] Avinash, K. Theory of charged dust clouds: Equilibrium. *Physics of Plasmas*, 14: 012904. 1-8, 2007.
- [3] Pandey, B. P., Vranješ, J., Poedts, S., and Shukla, P. K. The pulsational mode in the presence of dust charge fluctuations. *Physica Scripta*, 65: 513-517, 2002.
- [4] Bellan, P. M. Enrichment of the dust-to-gas mass ratio in Bondi/Jeans accretion/cloud systems due to unequal changes in dust and gas incoming velocities. *Astrophysical Journal*, 678: 1099-1108, 2008.
- [5] Tricco, T. S., Price, D. J., and Laibe, G. Is the dust-to-gas ratio constant in molecular clouds? *Monthly Notices of the Royal Astronomical Society*, 471: L52-L56, 2017.

- [6] Jeans, J. H. The stability of a spherical nebula. *Philosophical Transactions of the Royal Society*, 199: 1-53, 1902.
- [7] Avinash, K. Avinash-Shukla mass limit for the maximum dust mass supported against gravity by electric fields. *Journal of Plasma Physics*, 76: 493-500, 2010.
- [8] Avinash, K. and Gaurav, S. Equilibrium and stability of a gravitationally bound uniformly charged dust cloud. *Physics of Plasmas*, 24: 053703. 1-5, 2017.
- [9] Karmakar, P. K. and Borah, B. Nonlinear pulsational eigenmodes of a planar collisional dust molecular cloud with grain-charge fluctuation. *European Physical Journal D*, 67: 187. 1-14, 2013.
- [10] Borah, B. and Karmakar, P. K. Pulsational mode fluctuations and their basic conservation laws. *Advances in Space Research*, 55: 416-427, 2015.
- [11] Borah, B. and Karmakar, P. K. A theoretical model for electromagnetic characterization of a spherical dust molecular cloud equilibrium structure. *New Astronomy*, 40: 49-63, 2015.
- [12] Slattery, W. L, Doolen, G. D., and DeWitt, H. E. Improved equation of state for the classical one-component plasma. *Physical Review A*, 21: 2087-2095, 1980.
- [13] Donkó, Z. and Nyiri, B. Molecular dynamics calculation of the thermal conductivity and shear viscosity of the classical one-component plasma. *Physics of Plasmas*, 7: 45-50, 2000.
- [14] Karmakar, P. K. and Das, P. Stability of gravito-coupled complex gyrotory astrofluids. *Astrophysics and Space Science*, 362: 115. 1-9, 2017.
- [15] Brevik, I. Temperature variation in the dark cosmic fluid in the late universe. *Modern Physics Letters A*, 31: 1650050. 1-12, 2016.
- [16] Das, P. and Karmakar, P. K. Instability behaviour of cosmic gravito-coupled correlative complex bi-fluidic admixture. *Europhysics Letters*, 120: 19001. p1-p7, 2017.
- [17] Dutta, P. and Karmakar, P. K. Viscoelastic pulsational mode. *Astrophysics and Space Science*, 362: 141. 1-12, 2017.
- [18] Karmakar, P. K. and Das, P. Instability analysis of cosmic viscoelastic gyro-gravitating clouds in the presence of dark matter. *Astrophysics and Space Science*, 362: 142. 1-13, 2017.
- [19] Goutam, H. P. and Karmakar, P. K. Dynamics of streaming instability with quantum correction. *Journal of Physics: Conference Series*, 836: 012004. 1-4, 2017.



- [20] Karmakar, P. K. and Sarma, P. A non-ideal MHD model for structure formation. *Europhysics Letters*, 121: 35001. p1-p5, 2018.
- [21] Bastrukov, S. I., Weber, F., and Podgajny, D. V. On the stability of global non-radial pulsations of neutron stars. *Journal of Physics G: Nuclear and Particle Physics*, 25: 107-127, 1999.
- [22] Verheest, F. *Waves in Dusty Space Plasmas*. Kluwer Academic Publishers, London, 2000.
- [23] Spitzer Jr, L. *Physical Processes in the Interstellar Medium*. Wiley, New York, 2004.
- [24] Chandrasekhar, S. *Hydrodynamic and Hydromagnetic Stability*. Clarendon Press, Oxford, 1961.
- [25] Karmakar, P. K. and Borah, B. Global gravito-electrostatic fluctuations in self-gravitating spherical non-uniform charged dust clouds. *Astrophysics and Space Science*, 361: 115. 1-22, 2016.
- [26] Avinash, K., Eliasson, B., and Shukla, P. K. Dynamics of self-gravitating dust clouds and the formation of planetesimals. *Physics Letters A*, 353: 105-108, 2006.
- [27] Elmore, W. C., and Heald M. A., *Physics of Waves*. Dover, New York, 1969.
- [28] Karmakar, P. K. and Das, P. Nucleus-acoustic waves: Excitation, propagation, and stability. *Physics of Plasmas*, 25: 082902. 1-7, 2018.
- [29] McKelvey, J. P. Simple transcendental expressions for the roots of cubic equations. *American Journal of Physics*, 52: 269-270, 1984.
- [30] Larson, R. B. The physics of star formation. *Reports on Progress in Physics*, 66: 1651-1697, 2003.
- [31] Mac Low, M.-M. and Klessen, R. S. Control of star formation by supersonic turbulence. *Reviews of Modern Physics*, 76: 125-194, 2004.
- [32] Federrath, C. The role of turbulence, magnetic fields and feedback for star formation. in *Journal of Physics: Conference Series*, 719: 012002. 1-9, 2016.
- [33] Hennebelle, P. and Inutsuka, S.-I. The role of magnetic field in molecular cloud formation and evolution. *Frontiers in Astronomy and Space Sciences*, 6: 5. 1-30, 2019.
- [34] Karmakar, P. K. and Kalita, D. Dynamics of gravitational instability excitation in viscoelastic polytropic fluids. *Astrophysics and Space Science*, 363: 239. 1-11, 2018.

- [35] Tsytovich, V. N. Dust plasma crystals, drops, and clouds. *Physics-Uspekhi*, 40: 53-94, 1997.
- [36] Popel, S. I., Tsytovich, V. N., and Yu, M. Y. Shock structures in plasmas containing variable-charge macro particles. *Astrophysics and Space Science*, 256: 107-123, 1997.
- [37] Popel, S. I. and Tsytovich, V. N. Shocks in space dusty plasmas. *Astrophysics and Space Science*, 264: 219-226, 1998.
- [38] Vieillefosse, P. and Hansen, J. P. Statistical mechanics of dense ionized matter. v. hydrodynamic limit and transport coefficients of the classical one-component plasma. *Physical Review A*, 12: 1106-1116, 1975.
- [39] Hansen, J. P. Statistical mechanics of dense ionized matter. I. Equilibrium properties of the classical one-component plasma. *Physical Review A*, 8: 3096-3109, 1973.
- [40] Hu, R.-Y. and Lou, Y.-Q. Self-similar polytropic champagne flows in H II regions. *Monthly Notices of the Royal Astronomical Society*, 390: 1619-1634, 2008.
- [41] Durrive, J.-B. and Langer, M. Analytic growth rate of gravitational instability in self-gravitating planar polytropes. *Journal of Fluid Mechanics*, 859: 362-399, 2019.
- [42] Igochine, V. *Active Control of Magneto-hydrodynamic Instabilities in Hot Plasmas*. Springer, New York, 2015.
- [43] Dasgupta, S. and Karmakar, P. K. The Jeans instability in viscoelastic spherical astrophysical fluid media. *Astrophysics and Space Science*, 364: 213. 1-7, 2019.
- [44] Dutta, P. and Karmakar, P. K. Dynamics of gravoviscothermal instability in complex astrofluids amid cosmic radiative moderation effects. *Astrophysics and Space Science*, 364: 217. 1-8, 2019.
- [45] Hartquist, T. W. *Molecular Astrophysics*. Cambridge University Press, Cambridge, 1990.
- [46] Schwalbe, L. and Grilly, E. Thermal expansion of liquid normal hydrogen between 18.8 and 22.2 K. *Journal of Research of the National Bureau of Standards*, 89: 317-323, 1984.
- [47] Battaner, E. *Astrophysical Fluid Dynamics*. Cambridge University Press, Cambridge, 1996.
- [48] Harra, L. K. and Mason, K. O. *Space Science*. Imperial College Press, London, 2004.

- [49] Crutcher, R. M. Magnetic fields in molecular clouds. *Annual Review of Astronomy and Astrophysics*, 50: 29-63, 2012.
- [50] Crutcher, R. M. Magnetic fields in molecular clouds: observations confront theory. *Astrophysical Journal*, 520: 706-713, 1999.
- [51] Bourke, T. L., Myers, P. C., Robinson, G., and Hyland, A. R. New OH Zeeman measurements of magnetic field strengths in molecular clouds. *Astrophysical Journal*, 554: 916-932, 2001.
- [52] Tomisaka, K. and Ikeuchi, S. Gravitational instability of isothermal gas layers- Effect of curvature and magnetic field. *Publications of the Astronomical Society of Japan*, 35: 187-208, 1983.
- [53] Frenkel, J. *Kinetic Theory of Liquids*. Oxford University Press, Oxford, 1946.
- [54] Schwenn, R. and Marsch, E. *Physics of the Inner Heliosphere, I. Large-Scale Phenomena*. Springer, New York, 1990.
- [55] Gombosi, T. I. *Physics of the Space Environment*. Cambridge University Press, Cambridge, 1998.
- [56] Karmakar, P. K., Goutam, H. P., Lal, M., and Dwivedi, C. B. Stability analysis of the Gravito-Electrostatic Sheath-based solar plasma equilibrium. *Monthly Notices of the Royal Astronomical Society*, 460: 2919-2932, 2016.

## APPENDIX-4.A

### MEANFLUIDIC MOMENTUM EQUATION

An astronomical star-forming situation of magnetized polytropic spherical viscoelastic cloud fluid is considered in the framework of multicomponent fluid formalism (electrons, ions, and dust grains) to be reduced into a mean hydrodynamic form. As a first step, it is intended to arrive strategically at a mean construct of the fluid momentum equations on an averaging process. The momentum equations describing the dynamics of the constitutive electrons, ions and dust grains forming the magnetized complex plasma fluid can respectively be given as

$$m_e n_e \frac{d\vec{v}_e}{dt} = -e n_e (\vec{E} + \vec{v}_e \times \vec{B}) - \vec{\nabla} P_e - m_e n_e (1 + \gamma T_e) \vec{\nabla} \psi, \quad (4.A1)$$

$$m_i n_i \frac{d\vec{v}_i}{dt} = e n_i (\vec{E} + \vec{v}_i \times \vec{B}) - \vec{\nabla} P_i - m_i n_i (1 + \gamma T_i) \vec{\nabla} \psi, \quad (4.A2)$$

$$m_d n_d \frac{d\vec{v}_d}{dt} = -e Z_d n_d (\vec{E} + \vec{v}_d \times \vec{B}) - \vec{\nabla} P_d - m_d n_d (1 + \gamma T_d) \vec{\nabla} \psi + \eta \nabla^2 \vec{v}_d + \left( \zeta + \frac{\eta}{3} \right) \vec{\nabla} (\vec{\nabla} \cdot \vec{v}_d), \quad (4.A3)$$

where  $d/dt = (\partial/\partial t + \vec{v} \cdot \vec{\nabla})$  is the Lagrangian time derivative (or the convective material derivative).  $m_{e,i,d}$  denotes the mass of the electrons, ions and dust particles, respectively.  $n_{e,i,d}$  and  $v_{e,i,d}$  be their corresponding number densities and velocities.  $\vec{E}$  and  $\vec{B}$  represent the electric field and the magnetic field due to the charged particles, respectively.  $Z_d = |q_d/e|$  is the electric charge number of the identical dust grains. It may be noted that  $Z_d = 10^1 - 10^2$  in the HI region,  $Z_d = 10^1 - 10^4$  in the HII region, and  $Z_d = 10^1 - 10^6$  in the planetary rings [3].

Now, the equations (4.A1)-(4.A3) are compiled together to remodel the multi-component fluid into a single component fluid to give mean momentum equation as

$$\begin{aligned} \frac{d}{dt} (m_e n_e \vec{v}_e + m_i n_i \vec{v}_i + m_d n_d \vec{v}_d) = & e (-n_e + n_i - Z_d n_d) \vec{E} + (-e n_e \vec{v}_e + e n_i \vec{v}_i - Z_d e n_d \vec{v}_d) \times \vec{B} \\ & - \vec{\nabla} (P_e + P_i + P_d) - (\rho_e + \rho_i + \rho_d) \vec{\nabla} \psi - \gamma (\rho_e T_e + \rho_i T_i + \rho_d T_d) \vec{\nabla} \psi \end{aligned}$$

$$+\eta \nabla^2 \vec{v}_d + \left( \zeta + \frac{\eta}{3} \right) \vec{\nabla} (\vec{\nabla} \cdot \vec{v}_d), \quad (4.A4)$$

which, in terms of the new meanfluidic parameters, can now be simplified as

$$\begin{aligned} \rho \frac{d\vec{v}}{dt} &= e(-n_e + n_i - Z_d n_d) \vec{E} + \vec{J} \times \vec{B} - \vec{\nabla} P - \rho(1 + \gamma T) \vec{\nabla} \psi + \eta \nabla^2 \vec{v} \\ &+ \left( \zeta + \frac{\eta}{3} \right) \vec{\nabla} (\vec{\nabla} \cdot \vec{v}). \end{aligned} \quad (4.A5)$$

As  $m_e, m_i \ll m_d$  asymptotically, we can write the meanfluidic material density approximately as  $\rho = (m_e n_e + m_i n_i + m_d n_d) \approx m_d n_d \approx \rho_d$ , as already defined in the analytic formalism. The meanfluidic constitutive particle mass, which is indeed the mass density-weighted average fluid particle mass, is mathematically defined as  $m = (\rho_e m_e + \rho_i m_i + \rho_d m_d) / \rho_d \approx m_d$ . The meanfluidic (bulk) flow velocity is given as  $\vec{v} = (\rho_e \vec{v}_e + \rho_i \vec{v}_i + \rho_d \vec{v}_d) / \rho_d \approx \vec{v}_d$ . The meanfluidic pressure can be additively given as  $P = P_e + P_i + P_d$ . The meanfluidic temperature for the asymptotic mass scaling law  $m_e, m_i \ll m_d$ ; which yields the corresponding material density scaling law as  $\rho_e, \rho_i \ll \rho_d$ , can be explicitly expressed in a well averaging form as  $T = (\rho_e T_e + \rho_i T_i + \rho_d T_d) / \rho_d \approx T_d$ . Likewise, the meanfluidic electric current density on the basis of the free ionic gas model is derived as  $\vec{J} = n_e(-e)\vec{v}_e + n_i(e)\vec{v}_i + n_d(-Z_d e)\vec{v}_d$ . Applying the electrical quasi-neutrality condition,  $e(n_e + Z_d n_d) = en_i$  (electric charge conservation law in a local form), and the Ampere circuital law,  $\vec{\nabla} \times \vec{B} = \mu_0 \vec{J}$  (magnetic field non-conservation law in a local form), we reduce meanfluidic equation (4.A5) as

$$\rho \frac{d\vec{v}}{dt} = \frac{1}{\mu_0} (\vec{\nabla} \times \vec{B}) \times \vec{B} - \vec{\nabla} P - \rho(1 + \gamma T) \vec{\nabla} \psi + \eta \nabla^2 \vec{v} + \left( \zeta + \frac{\eta}{3} \right) \vec{\nabla} (\vec{\nabla} \cdot \vec{v}). \quad (4.A6)$$

In a viscoelastic medium, as in the present meanfluidic case, equation (4.A6) is directly modified due to the strong collective Coulombic correlative effects of the long-range origin among the constituent heavier charged dust particles into a  $g$ -MHD form [53] cast as

$$\begin{aligned} &\left\{ 1 + \tau_m \left( \frac{\partial}{\partial t} + \vec{v} \cdot \vec{\nabla} \right) \right\} \left\{ \rho \left( \frac{\partial}{\partial t} + \vec{v} \cdot \vec{\nabla} \right) \vec{v} + \frac{c_s^2}{\Gamma} \vec{\nabla} \rho + \rho(1 + \gamma T) \vec{\nabla} \psi - \frac{1}{\mu_0} (\vec{\nabla} \times \vec{B}) \times \vec{B} \right\} \\ &= \eta \nabla^2 \vec{v} + \left( \zeta + \frac{\eta}{3} \right) \vec{\nabla} (\vec{\nabla} \cdot \vec{v}). \end{aligned} \quad (4.A7)$$

In our spherically symmetric geometry, the meanfluid flows along the radial direction in the presence of an azimuthal magnetic field. As a result, equation (4.A7) in the radial degree of freedom (1-D) is finally reduced to the following simplified form

$$\begin{aligned} & \left\{ 1 + \tau_m \left( \frac{\partial}{\partial t} + v_r \frac{\partial}{\partial r} \right) \right\} \left\{ \rho \left( \frac{\partial}{\partial t} + v_r \frac{\partial}{\partial r} \right) v_r + \frac{c_s^2}{\Gamma} \frac{\partial \rho}{\partial r} + \rho (1 + \gamma T) \frac{\partial \psi}{\partial r} + \frac{B_\phi}{\mu_0 r} \frac{\partial}{\partial r} (r B_\phi) \right\} \\ & = \left( \zeta + \frac{4}{3} \eta \right) \left( \frac{2}{r} \frac{\partial v_r}{\partial r} + \frac{\partial^2 v_r}{\partial r^2} \right) - 2 \left( \zeta + \frac{1}{3} \eta \right) \frac{v_r}{r^2}. \end{aligned} \quad (4.A8)$$

In addition, as the toroidal magnetic field ( $B_\phi$ ) circulates about the chosen axis of our coordination reference (z-axis), the magnetic force density, which is defined as the net Lorentz force ( $\vec{F}_L$ ) acting per unit volume ( $V$ ) of the fluid ( $\vec{f}_L$ ), can now be expressed as

$$\vec{f}_L = \frac{\vec{F}_L}{V} = \frac{1}{\mu_0} (\vec{\nabla} \times \vec{B}) \times \vec{B} = \frac{1}{\mu_0} (\vec{B} \cdot \vec{\nabla}) \vec{B} - \vec{\nabla} \left( \frac{B^2}{2\mu_0} \right), \quad (4.A9)$$

where, all the symbols used herein carry the customary significances (as pre-defined). The first term on the right hand side of equation (4.A9) represents the ‘‘hoop stress’’, which arises due to the geometric curvature of the magnetic field lines [42, 48], acting radially inward (cloud-centric). The second term in the above represents the magnetic pressure gradient, acting radially outward in the anti-cloud-centric direction. This magnetic pressure gradient actually arises due to the spatial inhomogeneities of the magnetic field lines in the considered vast astrofluid [42, 48].

In this proposed theoretical study, we have adopted an astronomical viscoelastic self-gravitating cloud fluid configuration in the fabric of meanfluidic formalism in a spherically symmetric geometry on the Jeans spatiotemporal scales. It, hereby, enables us to stick only to a radial degree of freedom by ignoring any contribution in the basic mathematical formulation arising from the polar and azimuthal degrees of freedom judiciously; which might be, otherwise, accountable for the non-radial force field effects and subsequent non-radial fluctuations. So, the radial component of the magnetic force density sourced by the net magnetic field  $\vec{B} = (0, 0, B_\phi)$  from equation (4.A9) in the spherically symmetric geometry can be procedurally derived and written in the form as

$$f_{L,r} = \left\{ \frac{1}{\mu_0} (\vec{\nabla} \times \vec{B}) \times \vec{B} \right\}_r = -\frac{1}{\mu_0} \frac{B_\phi^2}{r} - \frac{\partial}{\partial r} \left( \frac{B_\phi^2}{2\mu_0} \right). \quad (4.A10)$$

In a normal spherically symmetric distribution of an ionized fluid matter on the astronomical spatiotemporal scales, the azimuthal (toroidal) magnetic field component is

well-known to decrease radially outward as  $B_\phi \propto r^{-1}$ ; whereas, the radial field component decreases as  $B_r \propto r^{-2}$  [54, 55]. The net magnetic field  $\vec{B} = (0, 0, B_\phi)$  in our case gets naturalistically auto-transformed purely into an azimuthal form as we move radially outward. In that case, the resultant Lorentz force contribution with the adopted field  $B_\phi = b/r$  in the corresponding effective magnetic force density in equation (4.A10) is seen to vanish subsequently as

$$f_{L,r} = -\frac{1}{\mu_0} \frac{b^2}{r^3} - \left( -\frac{1}{\mu_0} \frac{b^2}{r^3} \right) = 0, \quad (4.A11)$$

where,  $b$  is a proportionality constant signifying the strength of  $B_\phi$ . This is the equilibrium defined in the magnetized force-free meanfluidic configuration, and subsequently, the hydrostatic homogeneous equilibrium configuration well applies herein [48]. Such an equilibrium is termed as the “magnetohydrostatic homogeneous equilibrium” in the presented investigation, without any loss of generality. It, hereby, paves the way for a normal local mode analysis around the defined homogeneous equilibrium.

If we decompose the Lorentz force in equation (4.A8), in the special cases other than  $B_\phi \propto r^{-1}$ ; then, clearly, the finite non-zero contribution of this magnetic force enters the fluid equilibrium dynamics via the magnetic pressure gradient effects (by the last term in equation (4.A9)). So, the equilibrium gets transformed into a non-uniform inhomogeneous one (non-static type). It enables us to treat the meanfluidic equilibrium as the “magnetohydrodynamic inhomogeneous equilibrium”. It necessitates a judicious application of a normal non-local mode analysis, also termed as the eigen-value treatment [25, 41, 56], amid the real analytic complications of spatial inhomogeneties induced by the diversified equilibrium gradient forces.